Resonance Techniques For Inductive Sensor Applications

N.Kontos, L.Theodorakis, E.Hristoforou

Laboratory of Physical Metallurgy, School of Mining and Metallurgy Engineering, National Technical University of Athens, Zografou Campus, Athens 15780, Greece, eh@metal.ntua.gr

Abstract- This presentation describes the block diagram, explains the principal idea and shows the experimental results of a displacement and stress sensor. Both applications are based on inductive effects, while the examination of the sensor response determines the dependence of the permeability for all the different tested materials (magnetic cores) on the excitation frequency, the applied stress and the displacement of the material.

1. Introduction

The oncoming of inductive sensoring [1,2] with it's applications resulted in the advent of a new idea in the field of measuring methods along with the already existing such as the linear magnetostrictive displacement sensors [3,4] or sensors based on the magnetostrictive delay line technique [5]. A magnetic core is placed in a specifically designed solenoid and it's displacement (displacement sensor) or applied stress (stress sensor) has an effect on the inductance of the solenoid. Therefore, by placing the solenoid as a component of a RLC circuit, we can easily detect the displacement or the stress applied on the magnetic core by measuring the peak-to-peak voltage at the ends of the resistance R of the circuit. In order to attain the wanted results, the circuit needs to be supported by a generator and an oscillator. The former will provide us with the needed current for the electronic circuit giving us also the ability to investigate the sensor response with respect to different frequencies and the latter will give us the output signal (V_R).
As far as the displacement sensor is concerned the material used as the magnetic core was soft ferrite with chemical type $NiO{\cdot}Fe_2O_3$. For the stress sensor the material chosen was $Fe_{78}Si_7B_{15}$ (ribbon), due to it's remarkable magnetoelastic properties and sensitivity characteristics. The materials were also tested with respect to technical aging, so as to investigate their behavior after they were subjected to different treatments (annealing, corrosion, oxidation) or a combination of them. Finally, the dependence of permeability (μ) of the materials in relation to the displacement or stress in the inductance coil and the resonant frequency is examined. This examination refers again on samples subjected to treatments.

II. Displacement sensor

The block diagram shown in figure 1 illustrates the complete setup of the sensor including the RLC circuit, the function generator and the oscillator needed to attain the experimental results. It is illustrated how the ferrite is located in the setup, always bearing in mind that this is the moving element of the displacement sensor. The ferrite used was 14 cm long and the coil a two-layers solenoid, 25 cm in length, 2500 turns per layer (0,1 mm wire).
Transmitting voltage in a RLC circuit the resonant frequency of the circuit can be determined with respect to the displacement of the ferrite core of the coil. The voltage across the resistor R is given by:

$$V_R(t)=\frac{V_{\max}R}{\sqrt{R^2+\left(\frac{1}{\omega C}-\omega L\right)^2}}\sin\left(\omega t+\phi+\tan^{-1}\frac{\left(\frac{1}{\omega C}-\omega L\right)}{R}\right) \quad (1)$$

Accordingly, the inductance L is dependent on the permeability of the solenoid:

$$L=\mu N^2\frac{S}{\ell} \quad (2)$$

The sensor's response is attributed to the linear variation of the induction L occurring when the ferrite changes position into the solenoid.

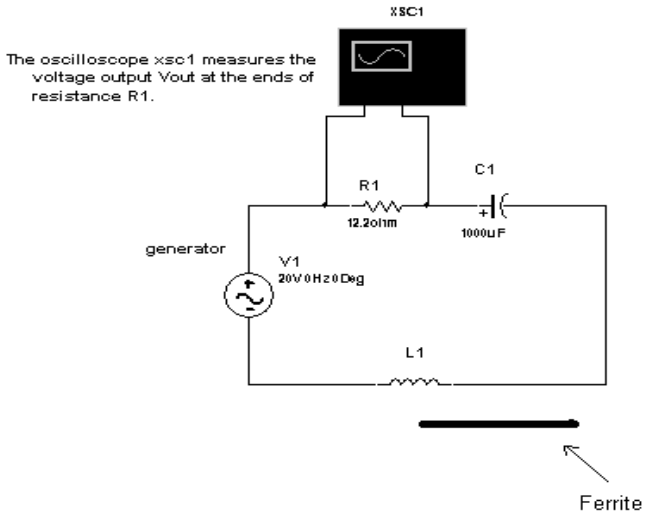

Figure 1. The block diagram

According to the above mentioned qualitative explanation and provided that the ferrite is magnetically uniform, the sensor's response for this experimental setup was determined:

$$L_x = l + (\mu - 1).\chi.\left(\mu_0 \mathrm{N}^2.\frac{S}{l^2}\right) \quad (3)$$

where L_x is the induction of the coil changing values with respect to the displacement of the ferrite x. The treatments took place under specific conditions. Oxidation was obtained in a furnace for 1h, in a temperature of 350ºC. Concerning corrosion, solution of H_2SO_4 was used, with 96% p.v. and pH = 2. Finally, the apotatic annealing took place in an oven of inert atmosphere with gas argon for 2 hours in 500ºC and followed by slow cooling for 5 h, in the oven up to 200ºC. Figure 3 presents a lack of sensitivity for transposition of the ferrite core for 4 cm inside the inductor. Also, ferrite without being subjected to any treatment, shows a monotonic response of the output signal in comparison with peculiar non-monotonic responses of the signal when it is undergone treatments such as corrosion (figure 3), which have been explained by the fact that aging results in permeability decrease which in turn results in resonance as the non monotonic response areas. The dependence of the permeability of the spinel ferrite on the frequency and the technical aging is examined in figures 4-7. The good agreement of the results can promise satisfying results for the behavior of the material and in retrospect for the sensoring ability of the application. More specifically, such modeling indicated that the developed position sensors operate well even after hard technical aging, when they are far from resonance. The dependence of permeability on the resonant frequency is illustrated in figures 6,7. The waveforms depicted in the two figures are described by two different exponential equations.

$\mu(f) = e^{-0,3f} + 20,06$, for ferrites without treatments, (4)
$\mu(f) = e^{-0,35f} + 12,75$, for ferrites that have been annealed (5)

The differences in the parameters of the exponentional equation show the differences between treated and non-treated ferrites, as far as the change of permeability with respect to frequency is concerned.

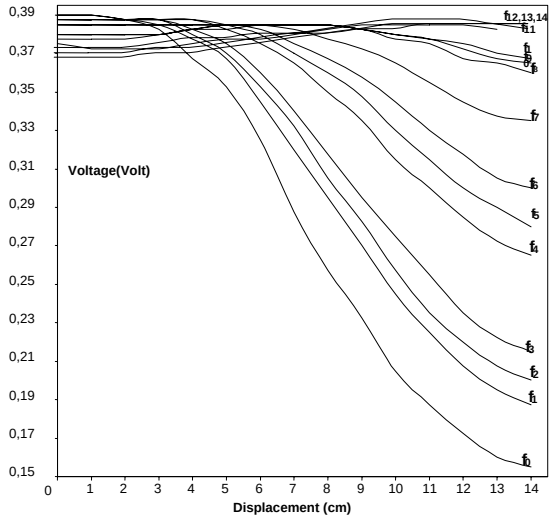

Figure 2. Ferrite without treatment

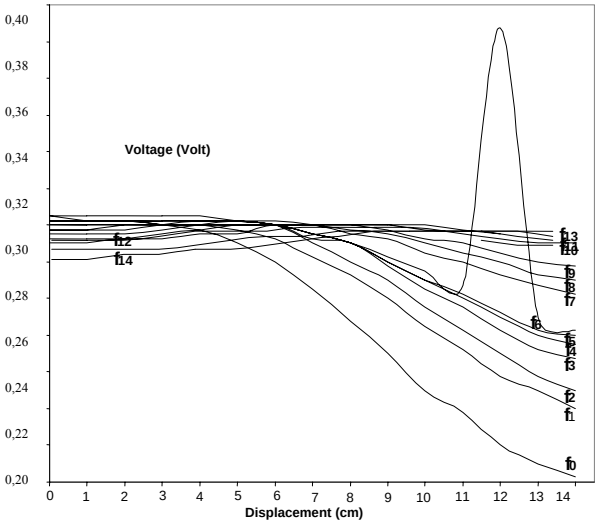

Figure 3. Ferrite corroded for 60 minutes

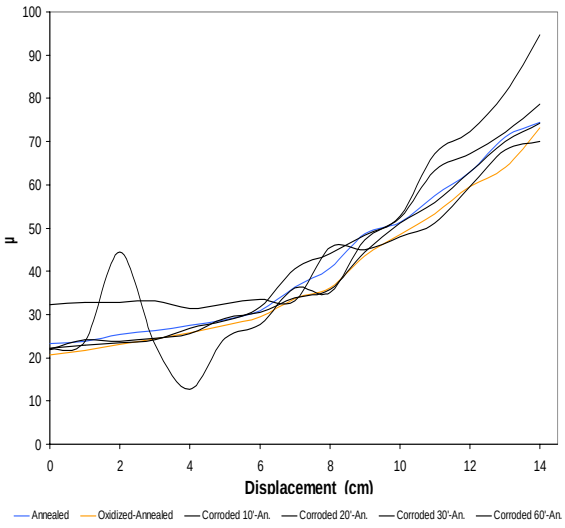

Figure 4. The change of permeability in relation to the displacement, for materials that have been annealed

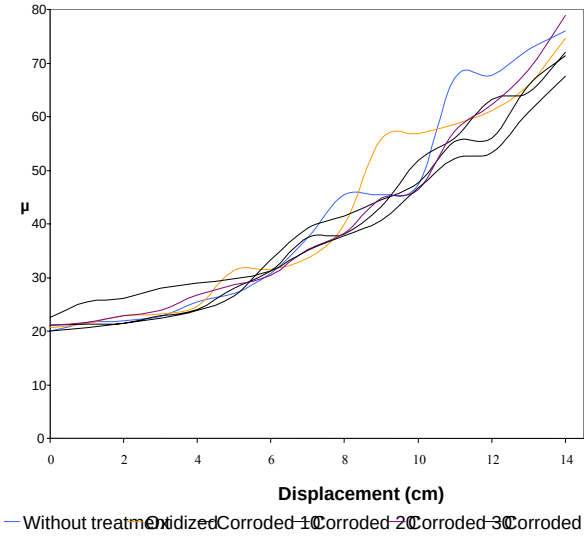

Figure 5. The change of the permeability in relation to the displacement of the ferrite

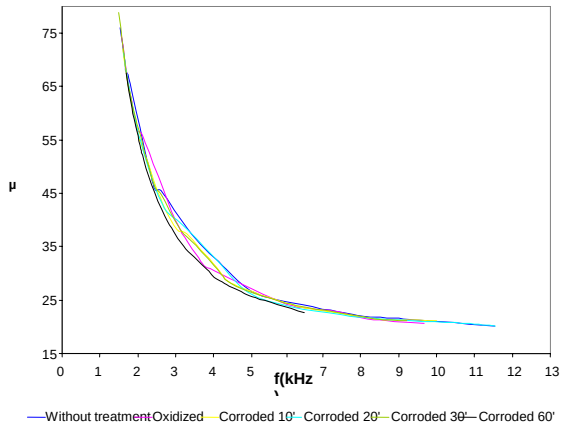

Figure 6. Dependence of the permeability on the resonant frequency

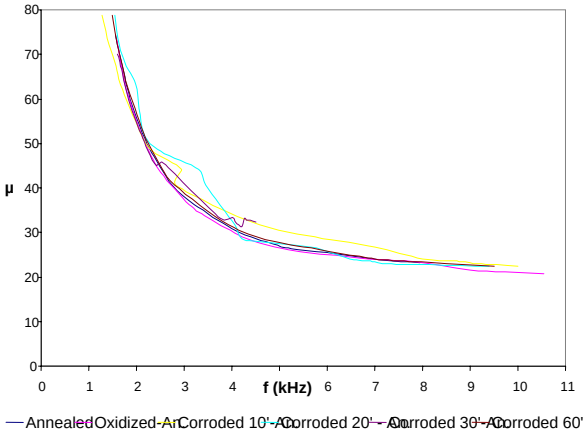

Figure 7. Dependence of the permeability on the resonant frequency for annealed materials

III. Stress sensor

The block diagram illustrates the components of the RLC circuit and the longitudinal direction of the stresses of the ribbon inside the coil.

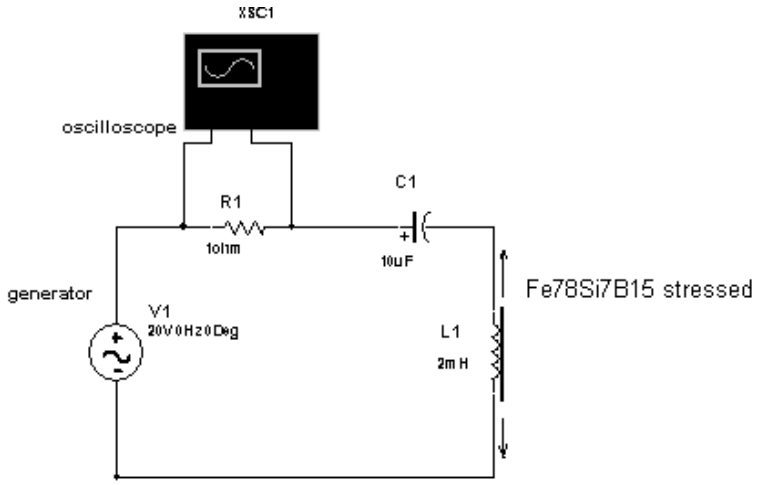

Figure 8. The block diagram of the stress sensor

The coil used is a two-layers solenoid, 25 cm in length, 2500 turns per layer (0,1 mm wire). The function generator enabled us to examine the sensor response with respect to a wide range of frequencies. The oscillator XSC1 is used to detect the peak-to-peak amplitude at the ends of resistance R. By applying longitudinal stresses on the material the inductance of the coil changes. The voltage across the resistor R is given by:

$$V_R(t) = \frac{V_{max} R}{\sqrt{R^2 + \left(\frac{1}{\omega C} - \omega L\right)^2}} \sin\left(\omega t + \phi + \tan^{-1}\frac{\left(\frac{1}{\omega C} - \omega L\right)}{R}\right) \quad (6)$$

while the inductance L is dependent on the permeability of the solenoid:

$$L = \mu N^2 \frac{S}{\ell} \quad (7)$$

Finally, the permeability (μ) of the coil alters with respect to the applied stress on the material:

$$\mu(\sigma) = Ae^{-Bt} + C \quad (8)$$

Feeding the circuit with different frequency currents, we examined the sensor response for several values, so as to make conclusions by investigating the parameters A, B, C of the exponentional equations that came up. The material $Fe_{78}Si_7B_{15}$ ribbon, was subjected to longitudinal stresses from 5-150 MPa. The sensor's response showed a monotonic dependence for all the tested frequencies. Two different families of responses have been determined, a monotonically rising (figure 9) and a monotonically falling one (figure 10).

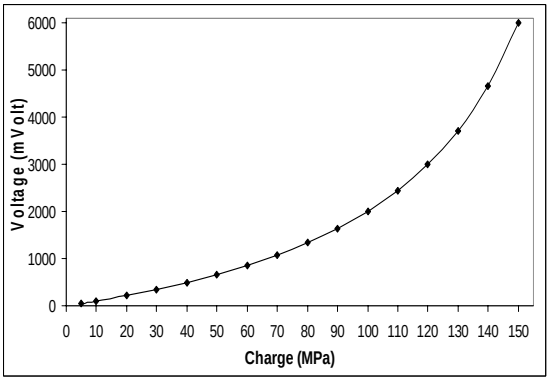

Figure 9. Voltage output with respect to charge (MPa). Rising response

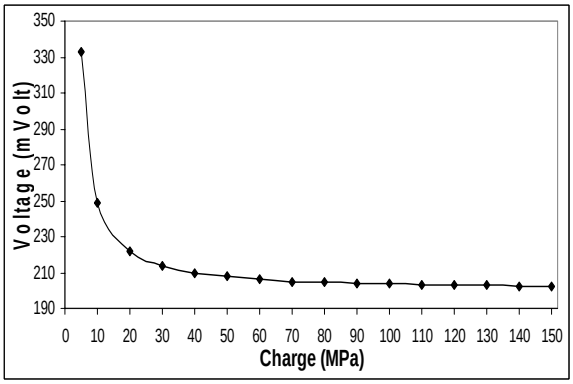

Figure 10. Voltage output with respect to charge (MPa). Falling response

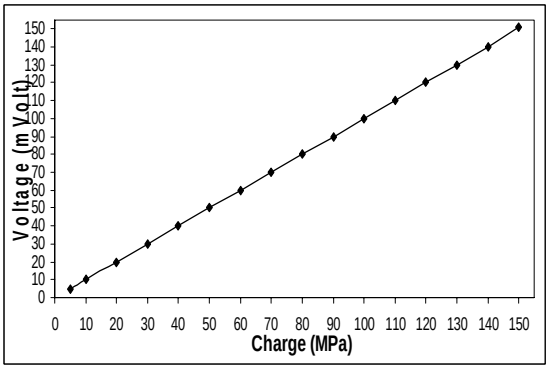

Figure 11. Voltage output with respect to longitudinal stress (MPa)

The figures above shown depict that the sensor characteristics have to be a compromise between linearity and sensitivity. Figure 11 shows great linearity for charges in the area of 5- 150 MPa.

On the other hand, sensitivity in figures 10 and 11 is significant. The parameter playing a vital role in this differentiation between samples is the excitation frequency. After close examination of the experimental results, the sensor performed excellent operation in frequencies between 10 and 100 KHz. More specifically, the parameters of the exponentional equation (8) were determined for frequencies of 1, 10 and 100 KHz.

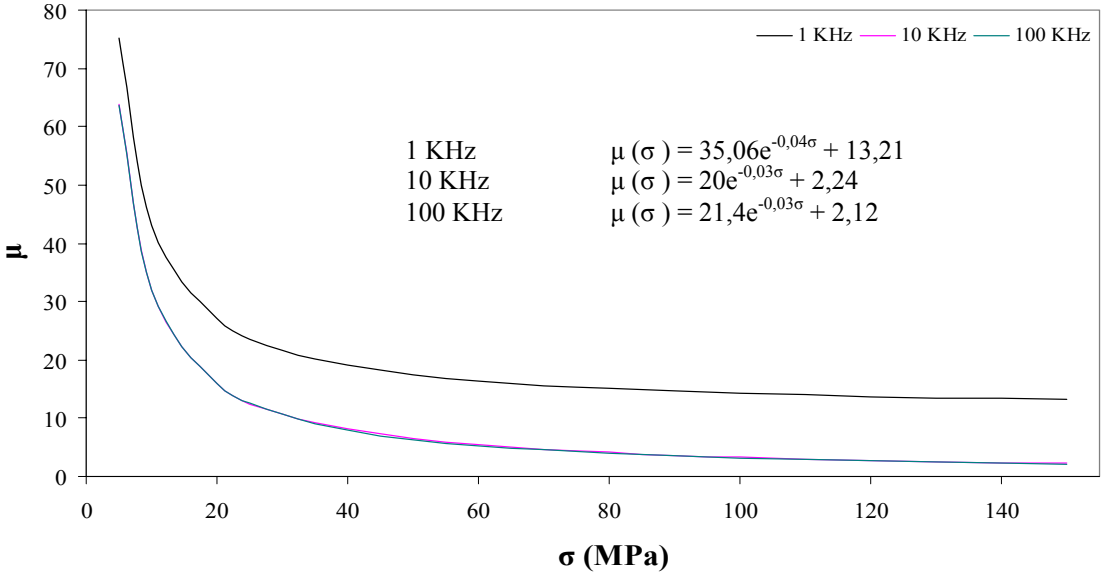

Figure 13. Change of permeability (μ) with respect to applied stress (MPa)

The change of permeability in figure 13 occurs for stress values between 10- 60 MPa. Also, we should note the similarities of the waveforms in figure 13, as far as frequencies 10 and 100 KHz are concerned.

References

[1] P. Kejik, K. Kluser, R. Bischofberger and R. S. Popovich, " A low-cost inductive proximity sensor for industrial applications ", *Sensors and Actuators A,* 110, 93-97, 2004.

[2] J. C. Butler, A. J. Vigliotti, F. W. Verdi and S. M. Walsh, " Wireless, passive, resonant circuit, inductively coupled, inductive strain sensor " , *Sensors and Actuators A,* 102, 61-66, 2002.

[3] R. Germano, G. Ausiano, V. Iannotti, L. Lannotte and C. Luponio, "Direct magnetostriction and magnetoelastic wave amplitude to measure a linear displacement ", *Sensors and Actuators A,* 81, 134-136, 2000.

[4] E. Hristoforou, D. Niarchos, "Amorphous wires in displacement sensing techniques", *Journal of Magnetism and Magnetic Materials,* 116, 177-188, 1992.

[5] E. Hristoforou, "Amorphous magnetostrictive wires used in delay lines in sensing applications", *Journal of Magnetism and Magnetic Materials,* 249, 387-392, 2002.

[6] D. de Cos, A. Garcia-Arribas and J. M. Barandiaran, "Simplified electronic interfaces for sensors based on inductance changes " , *Sensors and Actuators A,* 112, 302-307, 2004.